ChemComm

COMMUNICATION

View Article Online
View Journal | View Issue

Cite this: *Chem. Commun.*, 2023, 59, 14567

Received 22nd September 2023,
Accepted 10th November 2023

DOI: 10.1039/d3cc04723g

rsc.li/chemcomm

A Co(TAML)-based artificial metalloenzyme for asymmetric radical-type oxygen atom transfer catalysis†

Eva J. Meeus,[a] Nico V. Igareta,[b] Iori Morita,[b] Thomas R. Ward,*[b] Bas de Bruin*[a] and Joost N. H. Reek*[a]

We show that the incorporation of a biotinylated Co(TAML) cofactor within streptavidin enables asymmetric radical-type oxygen atom transfer catalysis with improved activity and enantioselectivity.

Artificial metalloenzymes (ArMs hereafter) are generated by anchoring a catalytically active non-natural metallocofactor within a protein host.[1,2] The unique combination of the synthetic tunability of the metallocofactors with the power of genetic engineering to evolve proteins, renders these systems highly attractive to access new-to-nature reactions.[3,4]

A variety of ArMs have been reported since the turn of the millennium.[1,2] These feature different non-natural metallocofactors and a handful of privileged protein scaffolds including carbonic anhydrase,[5] hemoproteins,[6] lactococcal multiresistance regulator,[7] serum albumins,[8] and (strept)avidin.[9] The resulting ArMs catalyse a broad range of reactions.[1] Non-natural metallocofactor-based ArMs that facilitate radical-type reactions; *i.e.*, proceeding *via* radical-type mechanisms[10–13] or intermediates,[14–16] have been reported as well, albeit less frequently.

From studies on ArM-catalysed transformations, it appears that the well-defined secondary coordination sphere around the metallocofactor provided by the protein may be tailored to optimise the activity and (enantio)selectivity of the corresponding ArM.[17,18] These hybrid catalysts thus combine attractive features of both homogeneous and enzymatic systems, thereby addressing some of the challenges typically associated with both fields.

In a recent study by the Ward group, the selective hydroxylation of benzylic C(sp^3)–H bonds was enabled by an artificial hydroxylase.[13] This ArM was assembled by anchoring a biotinylated Fe(TAML) complex (TAML = Tetra Amido Macrocyclic Ligand) into streptavidin (Sav hereafter) *via* the so-called biotin–streptavidin technology.[9] In addition to Fe(TAML) complexes, cobalt-based complexes (Co(TAML)) have been explored in oxygen atom transfer (OAT) catalysis,[19–21] albeit not yet within a protein host. Oxo and oxyl radical complexes can be generated using iodosylbenzene (PhIO),[19,21] *m*-CPBA,[20] or water and CAN.[21] These intermediates catalyse (radical-type) C–O and S–O bond formation, even in aqueous medium.[19,21]

Compared to iron-based systems, studies on cobalt-catalysed asymmetric OAT are limited and typically lead to moderate enantioselectivities. For example, the asymmetric epoxidation of styrenes, utilising chiral cobalt-based salen complexes[22] or anionic cobalt(III)-based complexes,[23,24] affords the respective epoxide products with 10–28% enantiomeric excess (ee hereafter). A first example of cobalt-catalysed asymmetric epoxidation affording ee's up to 94% was reported recently. In this study, a chiral cobalt-oxyl tetradentate complex was used to mediate oxygen atom transfer to olefins.[25]

To complement enantiopure ligand-design strategies, incorporation of an achiral cobalt-based cofactor within a host protein may offer an attractive strategy to achieve enantioselectivity for the above-mentioned reaction. Building on our recent report on the incorporation of biotinylated Fe(TAML) complexes within streptavidin,[13] we hypothesised that a similar strategy may enable the optimisation of enantioselective Co(TAML)-catalysed radical-type OAT reactions. Accordingly, we set out to (1) expand the scope of non-natural metallocofactors that enable ArM-catalysed radical-type transformations by incorporating a biotinylated Co(TAML) complex into Sav, (2) explore the performance of the resulting Co(TAML)-based ArM in asymmetric OAT catalysis, and (3) investigate the role of the secondary coordination sphere provided by Sav on the catalysis outcome. The key findings of this work are presented in Scheme 1.

The biotin–streptavidin technology capitalises on the remarkable affinity of biotin, and its derivatives, for Sav ($K_d \approx 10^{-14}$ M).[26] This affinity allows anchoring (almost) any

[a] *Van't Hoff Institute for Molecular Sciences (HIMS), University of Amsterdam (UvA), Science Park 904, Amsterdam 1098XH, The Netherlands. E-mail: b.debruin@uva.nl, j.n.h.reek@uva.nl*

[b] *Department of Chemistry, University of Basel, Mattenstrasse 22, Basel CH-4002, Switzerland. E-mail: thomas.ward@unibas.ch*

† Electronic supplementary information (ESI) available. See DOI: https://doi.org/10.1039/d3cc04723g

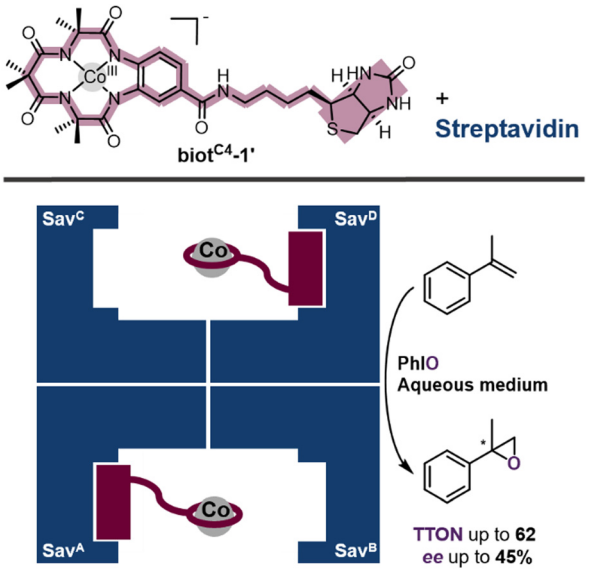

Scheme 1 Structure of the Co(TAML) cofactor (**biot^{C4}-1**′) and the schematic representation of the ArM resulting from anchoring **biot^{C4}-1**′ in Sav.

biotinylated probe within Sav. Importantly, the resulting homotetrameric Sav assembly remains remarkably stable against a variety of chaotropic factors, including extreme pH values, temperature, organic co-solvents, as well as mutagenesis.

To assemble the Co(TAML)-based ArM, a biotinylated TAML scaffold was synthesised[13] and metalated with cobalt (**biot^{C4}-1**′ in Scheme 1, see ESI† for more details; Scheme S1). Anchoring of the resulting Co(TAML)-based cofactor into Sav WT (wild type) was assessed using Isothermal Titration Calorimetry (Fig. S1, ESI†). A $K_d = 1.84 \times 10^{-8}$ M was derived, revealing a high affinity of the cofactor for Sav. Cofactor anchoring was further supported by a HABA displacement titration (Fig. S2, ESI†), which confirmed the incorporation of (up to) four cofactors into homotetrameric Sav. Eventually, **biot^{C4}-1**′·Sav WT was crystalised by sitting drop vapor diffusion (see ESI† for more details, Table S1). The resulting X-ray structure unambiguously confirmed the assembly of **biot^{C4}-1**′·Sav WT. Inspection of the X-ray structure (Fig. 1A) revealed that residues S112 and K121 lie closest to the cofactor.

Next, we evaluated the activity of the Co(TAML)-based ArM in OAT catalysis. Since homotetrameric Sav can host up to four cofactors, different cofactor : Sav ratios were initially explored, but no significant effects on the catalysis outcome were observed. We therefore selected the cofactor : Sav = 2 : 1 ratio as previously described for the biotinylated Fe(TAML) complexes for further experiments.[13] The artificial epoxidase was subjected to a reaction with 1 equivalent of iodosylbenzene as the *O*-source and 5 equivalents of α-methylstyrene in phosphate buffer (KPB) at pH 8 for 2 h (Table S2, ESI†).[13] Under these conditions, **biot^{C4}-1**′·Sav WT afforded (*R*)-α-methylstyrene oxide with 11% ee (total turnover number;[27,28] TTON = 32). In contrast, the free cofactor **biot^{C4}-1**′ afforded (*rac*)-α-methylstyrene oxide with a comparable TTON = 33. No product was observed in the absence of **biot^{C4}-1**′ or iodosylbenzene, confirming the involvement of the Co(TAML)-based cofactor and an *O*-source in the catalytic event (Table S2, entry 4 and 5, ESI†). Performing the reaction in $H_2{}^{18}O$ suggests that the formed oxo/oxyl radical intermediate likely undergoes exchange with water, as indicated by the incorporation of ^{18}O in the epoxide product (Fig. S5, ESI†).

To address the intermediacy of Co(TAML)-based oxyl radical complexes in the **biot^{C4}-1**′·Sav WT-catalysed epoxidation

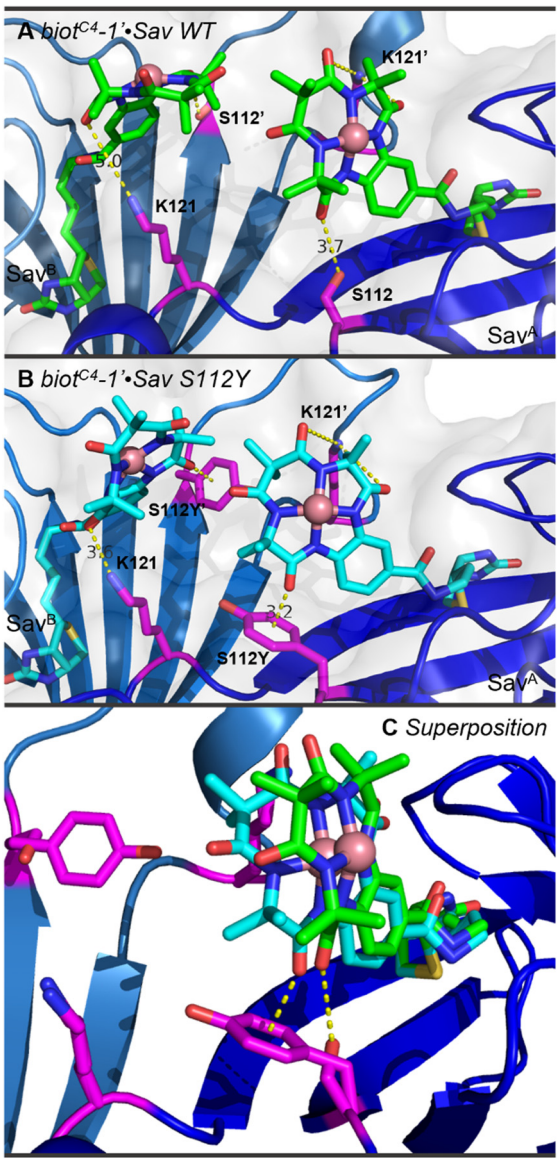

Fig. 1 Crystallographic characterisation of (A) **biot^{C4}-1**′·Sav WT (PDB: 8CRP), and (B) **biot^{C4}-1**′·Sav S112Y (PDB: 8CRN). The **biot^{C4}-1**′ cofactor is displayed as green (A) or cyan (B) sticks (atoms are colour-coded; nitrogen: blue, oxygen: red, carbon: green or cyan, chloride: green, and sulfur: yellow), and the cobalt centre as a pink sphere. The protein is displayed as a cartoon- and surface-accessible model. The monomers are colour-coded in different shades of blue. The residues S112 and K121 are displayed as purple sticks (atoms are colour-coded; nitrogen: blue, oxygen: red, and carbon: purple). The closest contacts with the cofactor are highlighted as a yellow dotted line, average distances in Å ((A) S112: ~3.7 Å, K121: ~5.0 Å; (B) S112Y: ~3.2 Å, K121: ~3.6 Å). The occupancy of the cobalt centre was set to 100%. (C) Superposition of both crystal structures (only one cofactor for each mutant is displayed for convenience).

reaction,[19] the above-described reaction was performed in the presence of the water-soluble radical trap 5,5-dimethyl-1-pyrroline *N*-oxide (DMPO; Table S2, entry 3, ESI†).[29] The addition of 5 equivalents of DMPO with respect to iodosylbenzene resulted in the formation of only traces of α-methylstyrene oxide. Given the known reactivity of DMPO as a radical scavenger, the negligible formation of epoxide product strongly supports the formation of radical-type intermediates in accordance with previous work.[19]

Next, we set out to improve the epoxidase activity of the ArM by genetically modifying the protein. In light of the proximity of both S112 and K121 residues to the Co(TAML)-moiety (Fig. 1A), we screened a focused library of single mutants at both these positions. The results are summarised in Scheme 2, using a colour code to display the selectivity while the size of the disk represents the TTON (Table S2, ESI†).

From these screening results based on purified Sav samples, the following features emerge:

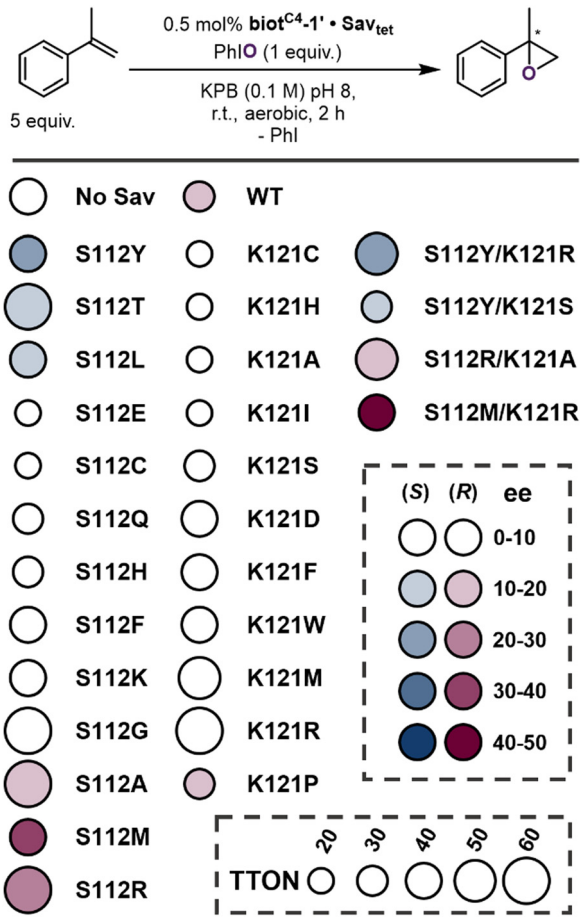

Scheme 2 Fingerprint summary of the Co(TAML)-catalysed epoxidation using iodosylbenzene (PhIO) as *O*-source (1 equiv.) and α-methylstyrene (5 equiv.) as prochiral substrate. Ratio **biot^{C4}-1′** : Sav = 2 : 1. TTON was determined after reaction completion by ^{1}H NMR integration using 1,3,5-tritertbutylbenzene as an external standard. The ee was determined by chiral GC-FID.

(1) Incorporation of **biot^{C4}-1′** into Sav samples with a single mutation at the S112 position can produce both (*R*)- and (*S*)-α-methylstyrene oxide, depending on the mutation.

(2) Substituting serine with methionine affords the highest selectivity for (*R*)-α-methylstyrene oxide (Sav S112M: 32% ee).

(3) Substituting serine with tyrosine affords the highest selectivity for (*S*)-α-methylstyrene oxide (Sav S112Y: 22% ee).

(4) Incorporation of **biot^{C4}-1′** into Sav samples with a single mutation at either or both the S112 and K121 positions can lead to increased TTONs.

(5) TTONs up to 62 were achieved by substituting serine with (a) arginine (Sav S112R: TTON = 55), (b) alanine (Sav S112A: TTON = 56) and (c) threonine (Sav S112T: TTON = 62). Substitution of lysine with methionine (Sav K121M: TTON = 52) and arginine (Sav K121R: TTON = 56) also resulted in increased TTONs.

(6) Incorporation of **biot^{C4}-1′** into Sav samples with a single mutation at the K121 position affords nearly racemic product, except mutant Sav K121P, which affords (*R*)-α-methylstyrene oxide with similar ee as observed for Sav WT.

The effect of **biot^{C4}-1′** anchoring into the Sav scaffold on the Co(TAML)-catalysed asymmetric epoxidation reaction was further explored in an additional control experiment (Table S2, entry 9, ESI†). We carried out the reaction using **biot^{C4}-1′** and Sav S112M spiked with 4 equivalents of biotin. Given the higher affinity of biotin over **biot^{C4}-1′** for Sav ($K_d = 10^{-14}$ M *vs.* 10^{-8} M, *vide supra*), the binding sites of the host protein are saturated with biotin, leaving the **biot^{C4}-1′** cofactor free in solution. As anticipated for this experiment, α-methylstyrene oxide was obtained in near racemic form (*i.e.*, 6% ee (*R*)), compared to 32% ee in the absence of biotin.

Finally, three of the most promising Sav single mutants, *i.e.*, Sav S112Y, S112R, and S112M, were combined with diverse mutants at position K121 (including hydrophobic, cationic and polar residues) (Scheme 2). From the four double mutants that were evaluated, **biot^{C4}-1′**·Sav S112Y/K121R afforded (*S*)-α-methylstyrene oxide with the highest ee (28%). **biot^{C4}-1′**·Sav S112M/K121R yielded the opposite enantiomer (*R*)-α-methylstyrene oxide with an improved ee (45%). These results highlight that the introduction of a well-structured secondary coordination sphere provided by Sav can be used to optimise the epoxidase activity of Co(TAML)·Sav ArMs, both in terms of activity (TTON up to 62) and selectivity (ee up to 45%).

Throughout screening, we did not observe a clear relationship between the nature of the amino acid residues and the observed enantioselectivities (including inversion). Hence, we set out to structurally characterise a genetically improved epoxidase variant to gain insight into structural details that may influence the enantioselectivity. Despite our efforts, we could not obtain the X-ray structure of the best double mutants. We could however solve the structure of **biot^{C4}-1′**·Sav S112Y (PDB: 8CRN) and compare it with **biot^{C4}-1′**·Sav WT (PDB: 8CRP) (Fig. 1). The structures of the host protein proved to be nearly superimposable, reflected by a Cα-RMSD = 0.130 Å. For both structures, the **biot^{C4}-1′** cofactor was modelled into the residual electron density from the biotin binding site with 100%

occupancy, supporting the localisation of the cofactor inside the Sav WT and Sav S112Y scaffolds.

Inspection of both X-ray structures (Fig. 1A, B and Fig. S3, ESI†) reveals the well-documented network of hydrogen bonds between the biotin moiety and the Sav binding site, further supporting the anticipated anchoring of the cofactor. The secondary coordination sphere around the Co(TAML) moiety of the cofactor was also carefully inspected. For **biot^{C4}-1′**·Sav WT specifically, the closest amino acids are Sav^{A} S112 (3.7–3.9 Å) and Sav^{B} K121′ (4.0–5.0 Å) (Fig. 1A, contacts highlighted with yellow dotted lines). These relatively long distances suggest limited interactions between these amino acids and the cofactor. Similar observations were made for **biot^{C4}-1′**·Sav S112Y. Based on the distance between the carbonyl moiety on the Co(TAML) scaffold and the amine residue of lysine (3.6–4.8 Å), no significant interactions with Sav^{B} K121′ are apparent. The absence of interactions between the cofactor and K121 residues is reflected in the outcome of the single mutant screening (*vide supra*). However, the mutation Sav S112Y (**biot^{C4}-1′**·Sav S112Y; Fig. 1B) affords a (slightly) different orientation of the cofactor, as highlighted by the superpositions of both ArMs (Fig. 1C and Fig. S4, ESI†). The short distance between the carbonyl moiety on the Co(TAML) scaffold and the aromatic center of the tyrosine residue (2.9–3.2 Å) suggests a n-π* interaction.[30] Such non-covalent interactions may force the Co(TAML) cofactor in a fixed conformation (Fig. 1B),[13] as has been previously observed for the analogues Fe(TAML)-based ArMs. Hence, we surmise that non-covalent interactions with close-lying amino acid residues may affect the catalysis outcome by affording a better-defined localisation of the cofactor, which could be a promising lead for further optimisation of such systems. It should be emphasised that the formation of the critical oxyl radical intermediate may significantly affect the position of the cofactor within the Sav mutants, which are not captured in the X-ray structures.

In conclusion, this study describes how incorporation of a biotinylated Co(TAML) cofactor within Sav enables asymmetric radical-type OAT catalysis. TTONs up to 62 and ee's up to 45% are achieved using Co(TAML)-based ArMs, representing an improvement in terms of activity and enantioselectivity upon the introduction of a well-structured secondary coordination sphere provided by Sav. Comparing the X-ray structures of two of these ArMs points towards the importance of non-covalent interactions. These interactions may affect the precise localisation and orientation of the cofactor, likely influencing the catalytic outcome. We envision that this rationale could guide further optimisation of catalytic systems to expand the scope of asymmetric radical-type OAT relying on cobalt-based ArMs.

Financial support from the research priority area Sustainable Chemistry of the University of Amsterdam and the Holland Research School of Molecular Chemistry PhD Mobility Program is gratefully acknowledged.

Conflicts of interest

There are no conflicts to declare.

Notes and references

1 F. Schwizer, Y. Okamoto, T. Heinisch, Y. Gu, M. M. Pellizzoni, V. Lebrun, R. Reuter, V. Köhler, J. C. Lewis and T. R. Ward, *Chem. Rev.*, 2017, **118**, 142–231.
2 F. Rosati and G. Roelfes, *ChemCatChem*, 2010, **2**, 916–927.
3 B. J. Bloomer, D. S. Clark and J. F. Hartwig, *Biochemistry*, 2022, **62**, 221–228.
4 K. Chen and F. H. Arnold, *Nat. Catal.*, 2020, **3**, 203–213.
5 F. W. Monnard, E. S. Nogueira, T. Heinisch, T. Schirmer and T. R. Ward, *Chem. Sci.*, 2013, **4**, 3269.
6 K. Oohora, A. Onoda and T. Hayashi, *Acc. Chem. Res.*, 2019, **52**, 945–954.
7 G. Roelfes, *Acc. Chem. Res.*, 2019, **52**, 545–556.
8 S. Eda, I. Nasibullin, K. Vong, N. Kudo, M. Yoshida, A. Kurbangalieva and K. Tanaka, *Nat. Catal.*, 2019, **2**, 780–792.
9 A. D. Liang, J. Serrano-Plana, R. L. Peterson and T. R. Ward, *Acc. Chem. Res.*, 2019, **52**, 585–595.
10 S. Lopez, D. M. Mayes, S. Crouzy, C. Cavazza, C. Leprêtre, Y. Moreau, N. Burzlaff, C. Marchi-Delapierre and S. Ménage, *ACS Catal.*, 2020, **10**, 5631–5645.
11 K. Renggli, M. G. Nussbaumer, R. Urbani, T. Pfohl and N. Bruns, *Angew. Chem., Int. Ed.*, 2013, **53**, 1443–1447.
12 Y. Miyazaki, K. Oohora and T. Hayashi, *Inorg. Chem.*, 2020, **59**, 11995–12004.
13 J. Serrano-Plana, C. Rumo, J. G. Rebelein, R. L. Peterson, M. Barnet and T. R. Ward, *J. Am. Chem. Soc.*, 2020, **142**, 10617–10623.
14 Y. Xu, F. Li, N. Zhao, J. Su, C. Wang, C. Wang, Z. Li and L. Wang, *Green Chem.*, 2021, **23**, 8047–8052.
15 S. Lopez, L. Rondot, C. Leprêtre, C. Marchi-Delapierre, S. Ménage and C. Cavazza, *J. Am. Chem. Soc.*, 2017, **139**, 17994–18002.
16 N. Fujieda, J. Schätti, E. Stuttfeld, K. Ohkubo, T. Maier, S. Fukuzumi and T. R. Ward, *Chem. Sci.*, 2015, **6**, 4060–4065.
17 J. Bos and G. Roelfes, *Curr. Opin. Chem. Biol.*, 2014, **19**, 135–143.
18 O. Pàmies, M. Diéguez and J.-E. Bäckvall, *Adv. Synth. Catal.*, 2015, **357**, 1567–1586.
19 E. J. Meeus, M. T. G. M. Derks, N. P. van Leest, C. J. Verhoef, J. Roithová, J. N. H. Reek and B. de Bruin, *Chem. Catal.*, 2023, **3**, 100700.
20 D. D. Malik, Y. Lee and W. Nam, *Bull. Korean Chem. Soc.*, 2022, **43**, 1075–1082.
21 S. Hong, F. F. Pfaff, E. Kwon, Y. Wang, M.-S. Seo, E. Bill, K. Ray and W. Nam, *Angew. Chem., Int. Ed.*, 2014, **53**, 10403–10407.
22 R. I. Kureshy, N. H. Khan, S. H. R. Abdi, A. K. Bhatt and P. Iyer, *J. Mol. Catal. A: Chem.*, 1997, **121**, 25–31.
23 K.-J. Kim, S.-W. Park and S. S. Yoon, *J. Korean Chem. Soc.*, 2000, **44**, 286–289.
24 S. Ozaki, H. Mimura, N. Yasuhara, M. Masui, Y. Yamagata, K. Tomita and T. J. Collins, J. Chem. Soc, *Perkin Trans*, 1990, **2**, 353–360.
25 Q. He, M.-P. Pu, Z. Jiang, H. Wang, X. Feng and X. Liu, *J. Am. Chem. Soc.*, 2023, **145**, 15611–15618.
26 M. E. Wilson and G. M. Whitesides, *J. Am. Chem. Soc.*, 1978, **100**, 306–307.
27 TTON refers to the total turnover number and includes the α-methylstyrene oxide product, quantified by ^{1}H NMR using 1,3,5-tritertbutylbenzene as an external standard. See ESI† for more details.
28 *Methods in Enzymology: AVidin-Biotin Technology*, ed. M. Wilchek, E. A. Bayer, Academic Press, San Diego, CA, 1990, vol. 184.
29 P. R. Marriott, M. J. Perkins and D. Griller, *Can. J. Chem.*, 1980, **58**, 803–807.
30 S. K. Singh and A. Das, *Phys. Chem. Chem. Phys.*, 2015, **17**, 9596–9612.

